

DOI: 10.1002/cbic.201300726

# Unique Crystal Structure of a Novel Surfactant Protein from the Foam Nest of the Frog *Leptodactylus vastus*

Denise Cavalcante Hissa,<sup>[a]</sup> Gustavo Arruda Bezerra,<sup>[b]</sup> Ruth Birner-Gruenberger,<sup>[c]</sup> Luciano Paulino Silva,<sup>[d]</sup> Isabel Usón,<sup>[e]</sup> Karl Gruber,<sup>\*,[b]</sup> and Vânia Maria Maciel Melo<sup>\*,[a]</sup>

Breeding by releasing eggs into stable biofoams ("foam nests") is a peculiar reproduction mode within anurans, fish, and tunicates; not much is known regarding the biochemistry or molecular mechanisms involved. Lv-ranaspumin (Lv-RSN-1) is the predominant protein from the foam nest of the frog *Leptodactylus vastus*. This protein shows natural surfactant activity, which is assumed to be crucial for stabilizing foam nests. We elucidated the amino acid sequence of Lv-RSN-1 by de novo sequencing with mass-spectrometry and determined the high-

resolution X-ray structure of the protein. It has a unique fold mainly composed of a bundle of 11  $\alpha$ -helices and two small antiparallel  $\beta$ -strands. Lv-RSN-1 has a surface rich in hydrophilic residues and a lipophilic cavity in the region of the antiparallel  $\beta$ -sheet. It possesses intrinsic surface-active properties, reducing the surface tension of water from 73 to 61 mN m<sup>-1</sup> (15  $\mu$ g mL<sup>-1</sup>). Lv-RSN-1 belongs to a new class of surfactants proteins for which little has been reported regarding structure or function.

## Introduction

Some amphibian species have developed a breeding strategy in which they deposit their eggs in environmentally stable foams in order to protect the eggs and developing larvae.<sup>[1]</sup> Interestingly, frog foam nests remain stable for long periods (in some cases more than one month) and are composed of a rich diversity of proteins termed ranaspumins (proteins from frog foam nests).<sup>[2-4]</sup>

From a biophysical point of view, the first step in the formation of a foam is to overcome the surface tension of the aqueous solution; thus foam nest production is only possible because of the presence of surfactant proteins.<sup>[3-5]</sup> Surfactants are

amphipathic compounds that act by decreasing surface and/or interfacial tension. Most known surfactants have lipid as the hydrophobic portion (nonpolar chain) and a hydrophilic portion (polar head). However, for surfactant proteins the boundaries of these two domains are not so obvious, and currently it is not well known how the structure of these surfactants behaves in interfacial or superficial surfaces.

Of the naturally occurring surfactant proteins,<sup>[6,7]</sup> ranaspumins constitute a particular case: they have the peculiar biological role of producing biofoams; they are not harmful to the eggs or sperm; and, their activity arises from their tertiary conformation and is independent of the presence of lipids.<sup>[5]</sup> As ranaspumins are intriguing proteins, not only for their exclusive and notable surfactant properties but also for their ecological roles in foam nests, we describe the amino acid sequence, crystal structure, and function of Lv-ranaspumin (Lv-RSN-1), a surfactant protein isolated from the foam nest of *Leptodactylus vastus*.

## Results and Discussion

### De novo sequencing

Lv-RSN-1 is a 23.5 kDa protein whose N-terminal amino-acid sequence was shown to be distinct from any previously reported protein sequence.<sup>[3]</sup> In this work, de novo sequencing of Lv-RSN-1 by MALDI-TOF/TOF achieved 97% coverage of the residues; the six C-terminal residues were deduced solely from the crystallographic electron density map. We used multiple enzymatic digests followed by nano-HPLC-MALDI tandem mass spectrometry to manually sequence 36 peptides de novo (Table S1 in the Supporting Information). Some of these fragments overlapped, thereby resulting in six larger peptides (17

[a] Dr. D. Cavalcante Hissa, Prof. Dr. V. M. Maciel Melo<sup>†</sup>  
Lab. de Ecologia Microbiana e Biotecnologia—LEMBiotech  
Departamento de Biologia, Universidade Federal do Ceará  
Av. Humberto Monte 2977, Campus do Pici, Bloco 909  
Fortaleza, CE, 60455-000 (Brazil)  
E-mail: vmmelo@ufc.br


[b] Dr. G. Arruda Bezerra, Prof. Dr. K. Gruber<sup>†</sup>  
Institute of Molecular Biosciences, University of Graz  
Humboldtstrasse 50/3, 8010 Graz (Austria)  
E-mail: karl.gruber@uni-graz.at

[c] Dr. R. Birner-Gruenberger  
Institute of Pathology, Medical University of Graz  
Center of Medical Research  
Omics Center Graz, Stiftingtalstrasse 24, 8010 Graz (Austria)

[d] Dr. L. Paulino Silva  
Laboratório de Espectrometria de Massa-LEM  
EMBRAPA Recursos Genéticos e Biotecnologia  
Parque da Estação Biológica, W5 Norte, Brasília, DF, 70770-917 (Brazil)

[e] Dr. I. Usón  
Instituto de Biología Molecular de Barcelona (IBMB-CSIC) and  
Institució Catalana de Recerca I Estudis Avançats  
Baldiri Reixach, 13-15, 08028 Barcelona (Spain)

[†] These authors contributed equally to this work.

 Supporting information for this article is available on the WWW under <http://dx.doi.org/10.1002/cbic.201300726>.

to 57 amino acid residues; Figure S1). The exact order of the peptides in the final sequence was only achievable by using the high resolution electron density map obtained by X-ray crystallography (see below).

The obtained sequence of Lv-RSN-1 showed 40% identity to ranaspumin-1 (Lf-RSN-1; GenBank: AAT66300),<sup>[2]</sup> a protein from the foam nest of *Leptodactylus fuscus*; its biological role has not been described. The second hit in the BLAST search was a protein of unknown function from *Bufo gargarizans*, an Asiatic toad (34% identity, 53% similarity). Other hits had higher *E* values ( $> 1 \times 10^{-4}$ ) and lower scores and query coverage.

### Structure of Lv-RSN-1

We crystallized Lv-RSN-1 under various conditions and obtained two crystal forms. The monoclinic crystal (space group  $P2_1$ ) diffracted to 1.6 Å and has one molecule in the asymmetric unit (37% solvent content according to the Matthews coefficient).<sup>[8,9]</sup> The orthorhombic crystal (space group  $P2_12_12_1$ ) also had one molecule in the asymmetric unit and diffracted to 1.75 Å (46% solvent content).

The lack of a complete amino acid sequence hampered the search for a reliable molecular-replacement model, and obtaining phases was problematic initially.<sup>[10]</sup> We solved the monoclinic structure by using ab initio phasing with the program ARCIMBOLDO,<sup>[11]</sup> which was facilitated by the predicted (and later confirmed) high  $\alpha$ -helical content. The resolution of the electron density was sufficient to identify most amino acids in the polypeptide chain; this helped in assembling the complete sequence, by grouping the peptides obtained by manual de novo sequencing. The orthorhombic structure was then solved by molecular replacement. Detailed statistics regarding data collection and structure refinement are shown in Table S2. Coordinates and structure factors have been deposited in the PDB under IDs 4K82 (monoclinic structure) and 4K83 (orthorhombic structure).

Despite the different packing, the overall structures of Lv-RSN-1 in the two crystals are very similar (RMSD 1.23 Å for 199 (out of 203) superimposed C $\alpha$ -atoms).

According to PISA analysis<sup>[12]</sup> Lv-RSN-1 is a monomer in the two crystal structures. It has a unique predominantly  $\alpha$ -helical structure: 11 helices and two small antiparallel  $\beta$ -strands. The structure can be described as being composed of two domains. The N-terminal half (up to approximately residue Leu121) forms a bundle of six antiparallel  $\alpha$ -helices, with the two shortest helices tilted with respect to the other four. The core of the C-terminal half (Asp122 onwards) is a sheet of three antiparallel helices with a fourth helix lying almost perpendicular to this group. The fold is stabilized by four disulfide bonds (Cys18–Cys67, Cys38–Cys114, Cys125–Cys168, Cys146–Cys207; Figure 1). There is no disulfide bond between the two protein halves.

Lv-RSN-1 was submitted to the CATHEDRAL server (<http://v3-4.cathdb.info/cgi-bin/CathedralServer.pl>), which uses structural comparison algorithms to identify domains already annotated in the CATH database. No statistically significant matches

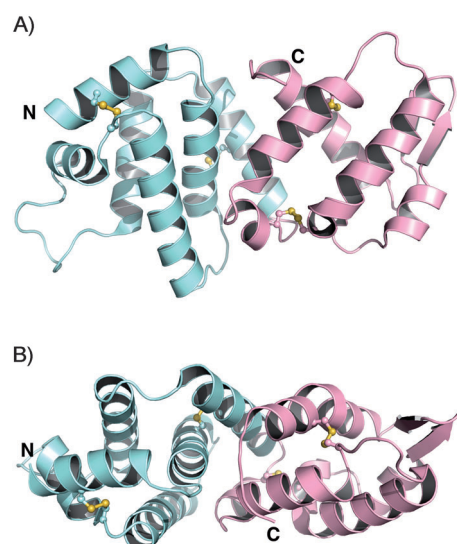


**Figure 1.** Overall structure of Lv-RSN-1 (PDB IDs: 4K82 and 4K83). A) Cartoon representation; cyan and pink differentiate the two halves of the protein; disulfides bridges are shown in yellow sticks; the letters N and C represent the respective termini of the protein. B) Orientation of the protein after rotation of 65° along the x-axis. The figure was generated by PyMol (DeLano Scientific, <http://www.pymol.org/>).

were found, thus indicating that Lv-RSN-1 represents a new fold.

Only two other protein structures from amphibian foam nests have been determined: Ep-RSN-2 (PDB ID: 2WGO) from *Engystomops pustulosus* and ranasmurfin (PDB ID: 2VH3) from *Polypedates leucomystax*, both very different in sequence and structure. Ep-RSN-2, the structure of which was determined by NMR, is an 11 kDa surfactant protein composed of four antiparallel  $\beta$ -strands with an  $\alpha$ -helix perpendicularly packed against the  $\beta$ -sheet.<sup>[13]</sup> The structure of ranasmurfin is mostly  $\alpha$ -helical and consists of a dimer (2  $\times$  13 kDa), covalently linked by an uncommon lysine tyrosyl quinone (LTQ) linkage with a blue-colored Zn chromophore.<sup>[14]</sup> The exact biological function of ranasmurfin, however, is still unknown.

### Surfactant activity

We measured the surfactant activity of purified Lv-RSN-1 by using the pendant drop shape approach and the Young–Laplace method in the *SCA20 (DataPhysics) analysis software* for analyzing the data. The protein effected a remarkable reduction in the surface tension of water. At 1.5 mg mL<sup>-1</sup>, the protein reduced the surface tension from (73.4  $\pm$  0.4) to (48.7  $\pm$  0.2) mN m<sup>-1</sup> (Figure 2). The minimum concentration at which Lv-RSN-1 effected a reduction was 15  $\mu$ g mL<sup>-1</sup> (from (73.4  $\pm$  0.4) to (61.7  $\pm$  2.2) mN m<sup>-1</sup>). Lysozyme (negative control) showed no effect on surface tension. In contrast, 1.5 mg mL<sup>-1</sup> BSA (a mild surfactant protein) reduced the surface tension of water to approximately 59 mN m<sup>-1</sup> (Figure 2). The crude foam fluid from which the protein Lv-RSN-1 was purified, also exhibited surfactant activity: surface tension reduced to approximately 54 mN m<sup>-1</sup> at a total protein concentration of 1 mg mL<sup>-1</sup>. In

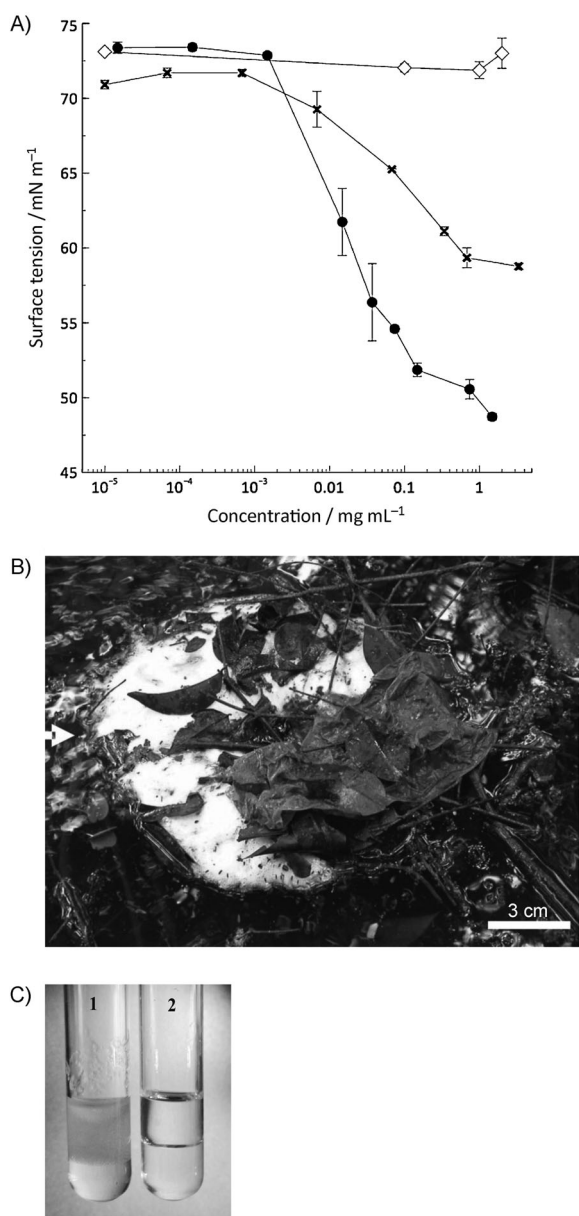


**Figure 2.** A) Surface tension versus concentration of Lv-RSN-1 from *L. vastus* (●), the lysozyme (negative control, ◇) and BSA (moderate surfactant control protein, ×). B) Foam nest from the frog *L. vastus*. C) Emulsification activity of Lv-RSN-1 (0.1 mg mL<sup>-1</sup>; 1) and water (negative control, 2).

contrast, size-exclusion chromatography fractions of this foam fluid corresponding to higher or lower molecular weight proteins did not show any significant reduction in surface tension. This suggests that Lv-RSN-1 is indeed the main surfactant protein in the foam nest.

Subsequently, the emulsification activity of the purified protein was tested: 0.1 mg mL<sup>-1</sup> was sufficient to exhibit an emulsification index of 35% against kerosene (Figure 2). Interestingly, the emulsion of the native protein was very stable for more than one month. CD spectroscopy analysis confirmed the stability of the protein: its fold was stable up to 95 °C, with only a small decrease in signal (208 nm) with increasing temperature. This property might be important, not only for the bio-

logical role of the protein, which needs to withstand environmental exposure, but also for potential industrial uses.

Interestingly size-exclusion chromatography and dynamic light scattering (DLS) demonstrated that the protein does not show any tendency to the formation of aggregates or oligomers in aqueous solution, and did not induce any micelle formation at either high or low concentrations. Self-assembly into micelles is a very common property of amphipathic molecules (hydrophobic portions form an inner core and hydrophilic portions in contact with the aqueous environment).<sup>[15]</sup>

The high solubility of Lv-RSN-1 in water is consistent with the large number of polar residues on the surface, showing a hydrophilic character. In addition it possesses remarkable surfactant activity: emulsifying a mixture of water in kerosene after agitation for two minutes. Also, when subjected to a RP-HPLC the protein strongly adsorbed at the stationary phase of a polystyrene-divinyl-benzene matrix; it eluted in 78% acetonitrile, thus showing also a hydrophobic character. For a molecule to act as an emulsifier it should be able to bring the polar phase into the nonpolar phase (or vice versa), so the molecule needs to be amphipathic.<sup>[16]</sup>

The structure of Lv-RSN-1 does not fully explain this peculiar activity or its duality. Hydrophobins from filamentous fungi are examples of surfactant proteins known to self-assemble; they form a hydrophobic patch covering ~20% of the surface area.<sup>[17]</sup> We did not observe a similar hydrophobic patch on Lv-RSN-1 when calculating the lipophilic potential at the surface of the Lv-RSN-1 with the program VASCO.<sup>[18]</sup> This analysis only revealed the presence of a lipophilic cavity, which might in part explain its surface-active properties (Figure 3).

Another speculation is that a conformational change in the protein is necessary to expose parts of the hydrophobic core to bind nonpolar molecules. Conformational changes have already been implicated in the surface-activity properties of latherin from horse sweat and saliva<sup>[19]</sup> as well as of Ep-RSN-2.<sup>[13]</sup> The structures of latherin and Ep-RSN-2 were reported to have uniformly polar surfaces, with no indication of any hydrophobic patch. Similarly to Lv-RSN-1, Ep-RSN-2 and latherin are well soluble and show no aggregation or micelle formation in solution.<sup>[13,19]</sup> The structure of Lv-RSN-1 allows at least two postulated conformational changes: movement between the two halves to expose the hydrophobic core of the protein; and, movement in the  $\beta$ -strands, thus increasing the lipophilic cavity (analysis with the programs SPIDER<sup>[20]</sup> and cons-PP1<sup>[21]</sup> predicted the  $\beta$ -strands as a possible region for protein interaction).

Even though micelle formation is not mandatory for a surfactant, it is surprising that ranaspumins act at the surface and form biobubbles but do not self-assemble in aqueous solution. We can only speculate that they might need contact with the nonpolar phase (e.g., air or a nonpolar solvent) together with some agitation for micelle formation; otherwise micelles would form inside the biological tissue where the protein is synthesized. Lv-RSN-1 is only beneficial to the frog when it forms a foam nest after it is secreted into the environment; it is known that male frogs use rapid motion of their legs as the agitation factor for beating the proteinaceous fluid released by



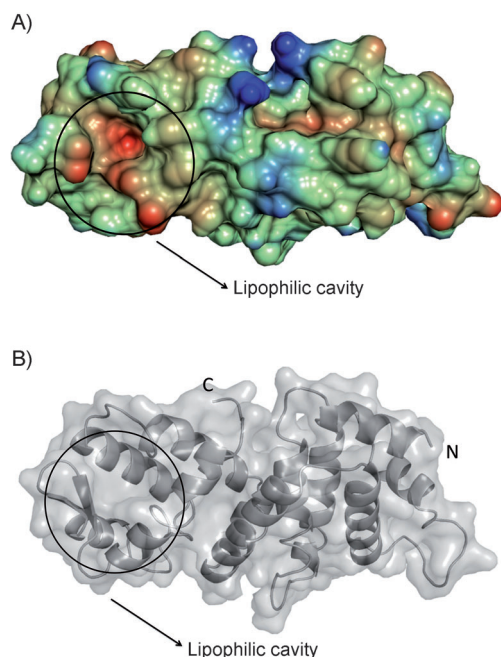


**Figure 3.** A) Surface representation of Lv-RSN-1 showing proposed hydrophobic cavity and lipophilic potential: hydrophobic (red), hydrophilic (blue). Calculations were done with the program VASCO. B) Cartoon representation of Lv-RSN-1 for better visualization of the proposed lipophilic cavity; N and C identify the respective termini of the protein. The figure was generated by PyMol (DeLano Scientific, <http://www.pymol.org/>).

the female, thus allowing the surfactant proteins to be in contact with the air (nonpolar phase) and forming the foam.

## Conclusions

The behavior of natural surfactant proteins is still not completely understood, but elucidation of the sequence and structure of Lv-RSN-1 allows new insights into the relationship between its structure and function. The sequence of the protein also enables future studies into the heterologous expression of the protein, the generation of variants, and functional classification. From a biotechnological perspective, Lv-RSN-1 has many potential applications thus presenting advantages over synthetic surfactants, such as superior biodegradability, lower toxicity, and better biocompatibility.

## Experimental Section

**Protein purification:** Foam nests of *L. vastus* were collected, and foam fluid was obtained according to a previously published procedure.<sup>[3]</sup> Foam nests were collected in Campus do Pici, Universidade Federal do Ceará, Brazil during the rainy season (March and April) of 2011 with proper regard to Brazilian legislation and ecological concerns (Permit of Instituto Brasileiro do Meio Ambiente e dos Recursos Naturais Renováveis—IBAMA 13587-1). Lv-RSN-1, the main protein in the nest, was purified according to Hissa et al.<sup>[10]</sup> After ion exchange (MonoQ 4.5/100, GE Healthcare; elution with a gradient of Tris-HCl (20 mM), NaCl (1 M)) and size-exclusion chromatography (HiLoad 26/60 Superdex 200, GE Healthcare; equilibrated with Tris-HCl (50 mM, pH 8.0), NaCl (100 mM)), the homo-

geneous protein (as assessed by SDS-PAGE) was concentrated (14.8 mg mL<sup>-1</sup>, based on colorimetric Bradford quantification<sup>[22]</sup>) for crystallization trials. Other proteins in the foam nest (higher and lower molecular-weight fractions from size-exclusion chromatography) were stored for use as negative controls in surface tension assays.

**Interfacial tension measurements:** A range of concentrations of Lv-RSN-1 (15 ng mL<sup>-1</sup> to 1.5 mg mL<sup>-1</sup>), bovine serum albumin (BSA; 0.01 μg mL<sup>-1</sup> to 3.3 mg mL<sup>-1</sup>; Sigma–Aldrich), Lysozyme (10 ng mL<sup>-1</sup> to 2 mg mL<sup>-1</sup>; Fluka) and the foam nest fluid (10 ng mL<sup>-1</sup> to 1.5 mg mL<sup>-1</sup>) diluted in ultrapure water were tested. The interfacial tension measurements were carried out by the pendant drop shape method: a drop is formed and illuminated by uniform light with a Contact Angle System OCA20 (DataPhysics OCA, Filderstadt, Germany) and its profile was imaged by a CCD camera. The shape and size of the drop formed at the tip of a needle fixed on a syringe were analyzed by the drop analysis software SCA20 (DataPhysics) with the Young–Laplace method. The inner diameter of the needle was 1.36 mm, and the volume of the droplet was ~20 μL, depending on the experimental conditions. The temperature was (20 ± 1) °C. Experimental error was estimated by the standard deviation from the mean of the triplicate measurements.

**Emulsification activity assay:** Emulsification activity of the protein was evaluated according to Iqbal et al.<sup>[23]</sup> with modifications. Briefly, purified protein (0.9 mL, 0.1 mg mL<sup>-1</sup>) was combined with the same volume of kerosene in a 10 mL tube, and mixed by using a vortex for 2 min, and left to stand for 24 h. Emulsification index (EI, %) was calculated from the equation EI = (height of emulsion layer/height of oil plus emulsion layer) × 100.

**Circular dichroism spectroscopy (CD) analysis:** Circular dichroism (CD) spectra were collected on a J-715 CD spectropolarimeter (JASCO, Tokyo, Japan; 208 nm). Thermostability of the secondary structure of purified Lv-RSN-1 (0.2 mg mL<sup>-1</sup>) was analyzed from 20 to 95 °C (0.2 °C increments).

**Crystallization:** First, crystals of Lv-RSN-1 had previously been obtained<sup>[10]</sup> at 293 K by sitting-drop vapor diffusion with an OryxNano crystallization robot (Douglas Instruments, Hungerford, UK). These crystals had grown under various conditions from the PEG/Ion-Screen (Hampton Research, Aliso Viejo, CA), and the first diffraction dataset was collected to a maximum resolution of 3.5 Å. At that time, a structure solution was not possible because of lack of the protein sequence and the low resolution of the dataset.

In the present study we re-examined initial crystals obtained under different conditions.<sup>[10]</sup> Sitting drop crystallization screens consisted of drops of protein solution (0.7 μL, 14.8 mg mL<sup>-1</sup>) in Tris-HCl (50 mM, pH 8.0) and NaCl (100 mM) mixed with the precipitant solution (0.7 μL) and equilibrated against the reservoir solution (70 μL). In this study two crystal forms were analyzed. Monoclinic crystals (small plate-like) grew within nine months under condition #22 (potassium formate (0.2 M), PEG 3350 (20%), pH 7.3). Orthorhombic crystals grew within two weeks under optimized conditions (sodium acetate (0.25 M) and PEG 3350 (28%)) by using hanging-drop vapor diffusion (equilibration in Linbro Plates of the protein solution (1 μL, 18.5 mg mL<sup>-1</sup>) and the precipitant solution (1 μL) against the reservoir solution (250 μL)), thereby yielding large and thick needles.

**Mass spectrometry/de novo sequencing:** Spots corresponding to Lv-RSN-1 were excised from SDS-PAGE gels,<sup>[24]</sup> destained, reduced with dithiothreitol (DTT), alkylated with iodoacetamide and dried for further enzymatic in-gel digestion. Digestions with trypsin

(Promega), Asp-N (Roche), chymotrypsin (Roche), Glu-C (New England BioLabs), and Lys-C (Promega) were performed following manufacturers' protocols. Digests proceeded overnight for complete hydrolysis or for 40 min for partial hydrolysis. Hydrolyzed peptides were extracted following published procedures<sup>[25]</sup> and subjected to reversed-phase nano liquid chromatography (LC) with a Zorbax 300SB-C<sub>18</sub> column (3.5  $\mu$ m, 150 mm  $\times$  75  $\mu$ m; Agilent) after online concentration and desalting on a Zorbax 300SB-C<sub>18</sub> enrichment column (5  $\mu$ m, 5  $\times$  0.3 mm; Agilent). Separation (flow rate 300 nL/min) was carried out with solvent A (TFA (0.1%, v/v)) and B (acetonitrile (80%) and TFA (0.1%, v/v)) with gradient: 0–29 min 13–28% B, 29–41 min 28–50% B, 41–42 min 50–100% B, 42–52 min 100% B, 52–53 min 100–13% B, 53–63 min 13% B. The nano LC was attached to a MALDI spotter (SunChrom, Friedrichsdorf, Germany); the mobile phase was sheathed with a matrix solution (800  $\mu$ L prepared from 748  $\mu$ L 95% acetonitrile, 0.1% TFA, 36  $\mu$ L saturated  $\alpha$ -cyano-4-hydroxycinnamic acid in 95% acetonitrile, 0.1% TFA, 8  $\mu$ L 10% TFA, 8  $\mu$ L 100 mM NH<sub>4</sub>H<sub>2</sub>PO<sub>4</sub>) at 100  $\mu$ L h<sup>-1</sup>. 15 s fractions corresponding to 75 nL analyte and 420 nL matrix were spotted onto a AnchorChip target plate (Bruker). Monoisotopic masses of molecular components were obtained in positive reflectron mode on MALDI TOF/TOF mass spectrometers UltraFlex III or Extreme (Bruker Daltonics) with external calibration by a suitable peptide calibration standard mixture (Bruker Daltonics). MS/MS spectra were obtained by LIFT/CID fragmentation and annotated manually by using FlexAnalysis 3.3 software (Bruker Daltonics).<sup>[26]</sup> The obtained amino acid sequences were subjected to automatic alignment (BLAST),<sup>[27]</sup> and to Biotools 3.2 software (Bruker Daltonics) for validation. The isobaric amino acids isoleucine and leucine could not be differentiated. Lysine and glutamine were also treated as isobaric amino acid residues; however, these were clearly differentiated in the structure determination step.

**Structure determination:** A first diffraction dataset from the monoclinic crystal was collected at beamline PXI of the Swiss Light Source (SLS) at the Paul Scherrer Institut (PSI); Villingen, Switzerland). This beamline was equipped with a CCD detector CHESS (Cornell University, High Energy Synchrotron Source), and we collected 270 images with a 1° oscillation and a crystal-to-detector distance of 150 mm. Data were processed in space group *P*<sub>2</sub><sub>1</sub> to 1.6 Å resolution by using the programs XDS<sup>[28]</sup> and SCALA.<sup>[29]</sup> The program POINTLESS was used to confirm the space group assignment.<sup>[29]</sup> Because CD data indicated that the protein was predominantly  $\alpha$ -helical (data not shown) and the crystal diffracted to a good resolution, we decided to test ab initio phasing; the phases were solved by using the program ARCIMBOLDO.<sup>[11]</sup> Portions of the electron density were interpreted from fragments of the de novo sequence of the protein, and residues missing from this sequence were deduced from the electron density where possible. The starting model was completed and refined by using the programs REFMAC, PHENIX, and COOT.<sup>[30–32]</sup> *R*<sub>free</sub> values were computed for 5% randomly chosen reflections not used for the refinement.

The second dataset, corresponding to the orthorhombic crystal form, was collected at the SLS-beamline PXIII equipped with a Pilatus 2M detector (Dectris, Baden, Switzerland). A total of 2880 images were collected with 0.25° oscillation and a crystal to detector distance of 220 mm. Data were processed in space group *P*<sub>2</sub><sub>1</sub><sub>2</sub><sub>1</sub> to 1.75 Å resolution. The structure was solved by molecular replacement with the program Phaser,<sup>[33]</sup> with the partially refined model obtained from the first dataset as template.

In both structures, only weak electron density was observed for a loop region around residue 80. Therefore, residues 79–82 are

missing in the monoclinic structure, and residues 79–81 are missing in the orthorhombic structure. The amino acid sequence of the six C-terminal residues was not elucidated by de novo sequencing, but was deduced from the electron density map. The final structures thus contain amino acids 13–217 (the first 12 residues in the N-terminal were apparently cleaved off either during the crystallization process).<sup>[10]</sup>

The stereochemistry of the structures was checked by using MOLPROBITY,<sup>[34]</sup> which showed only one Ramachandran outlier in each structure (Glu80 in the monoclinic and Leu78 in the orthorhombic structure). Both residues are located in the loop, for which only weak electron density was observed (see above). Details of the data collection, processing, and refinement are summarized in Table S2.

## Acknowledgements

We are grateful to Kay Diederichs for the help with the structure determination, Britta Obrist and Stefan Spoerk for technical assistance with LC-MALDI-TOF/TOF and Srinivasan Rengachari, Domen Zafred, Tea Pavkov-Keller and Paulo Cascon for the valuable discussions. We thank Volker Ribitsch for providing access to the Contact Angle System used in this work. We acknowledge Christine Orengo and Alison Cuff for further analyzing the protein fold. We also thank the staff at the Synchrotron SLS for the assistance in data collection. D.C.H. was recipient of a scholarship provided by Conselho Nacional de Desenvolvimento Científico e Tecnológico (CNPq; Process No. 201633/2012-8). This work was financially supported by Coordenação de Aperfeiçoamento de Pessoal de Nível Superior (CAPES), by CNPq and by the Austrian Science Funds (FWF) through project W901 (DK "Molecular Enzymology", to K.G.)

**Keywords:** amphibians · Lv-ranaspumin · mass spectrometry · structural biology · surfactants

- [1] W. R. Heyer, *Evolution* **1969**, *23*, 421–428.
- [2] R. I. Fleming, C. D. Mackenzie, A. Cooper, M. W. Kennedy, *Proc. R. Soc. London Ser. B* **2009**, *276*, 1787–1795.
- [3] D. C. Hissa, I. M. Vasconcelos, A. F. U. Carvalho, V. L. R. Nogueira, P. Cascon, A. S. Antunes, G. R. de Macedo, V. M. M. Melo, *J. Exp. Biol.* **2008**, *211*, 2707–2711.
- [4] A. Cooper, M. W. Kennedy, R. I. Fleming, E. H. Wilson, H. Videler, D. L. Wokosin, T.-j. Su, R. J. Green, J. R. Lu, *Biophys. J.* **2005**, *88*, 2114–2125.
- [5] A. Cooper, M. W. Kennedy, *Biophys. Chem.* **2010**, *151*, 96–104.
- [6] M. L. De Vocht, I. Reviakine, W.-P. Ulrich, W. Bergsma-Schutter, H. A. B. Wösten, H. Vogel, A. Brisson, J. G. H. Wessels, G. T. Robillard, *Protein Sci.* **2002**, *11*, 1199–1205.
- [7] K. B. Vargo, R. Parthasarathy, D. A. Hammer, *Proc. Natl. Acad. Sci. USA* **2012**, *109*, 11657–11662.
- [8] B. W. Matthews, *J. Mol. Biol.* **1968**, *33*, 491–497.
- [9] K. A. Kantardjieff, B. Rupp, *Protein Sci.* **2003**, *12*, 1865–1871.
- [10] D. C. Hissa, G. A. Bezerra, B. Obrist, R. Birner-Grünberger, V. M. M. Melo, K. Gruber, *Acta Crystallogr. Sect. F Struct. Biol. Cryst. Commun.* **2012**, *68*, 321–323.
- [11] D. Rodríguez, M. Sammito, K. Meindl, I. M. de Illarduya, M. Potratz, G. M. Sheldrick, I. Usón, *Acta Crystallogr. Sect. D Biol. Crystallogr.* **2012**, *68*, 336–343.
- [12] E. Krissinel, K. Henrick, *J. Mol. Biol.* **2007**, *372*, 774–797.
- [13] C. D. Mackenzie, B. O. Smith, A. Meister, A. Blume, X. Zhao, J. R. Lu, M. W. Kennedy, A. Cooper, *Biophys. J.* **2009**, *96*, 4984–4992.

- [14] M. Oke, R. T. Y. Ching, L. G. Carter, K. A. Johnson, H. Liu, S. A. McMahon, M. F. White, C. Bloch, C. H. Botting, M. A. Walsh, A. A. Latiff, M. W. Kennedy, A. Cooper, J. H. Naismith, *Angew. Chem.* **2008**, *120*, 7971–7974; *Angew. Chem. Int. Ed.* **2008**, *47*, 7853–7856.
- [15] R. M. Garavito, S. Ferguson-Miller, *J. Biol. Chem.* **2001**, *276*, 32403–32406.
- [16] T. Tadros, P. Izquierdo, J. Esquena, C. Solans, *Adv. Colloid Interface Sci.* **2004**, *108–109*, 303–318.
- [17] X. L. Zhang, J. Penfold, R. K. Thomas, I. M. Tucker, J. T. Petkov, J. Bent, A. Cox, I. Grillo, *Langmuir* **2011**, *27*, 10514–10522.
- [18] G. Steinkellner, R. Rader, G. G. Thallinger, C. Kratky, K. Gruber, *BMC Bioinf.* **2009**, *10*, 32.
- [19] S. J. Vance, R. E. McDonald, A. Cooper, B. O. Smith, M. W. Kennedy, *J. R. Soc. Interface* **2013**, *10*, 20130453.
- [20] A. Porollo, J. Meller, *Proteins Struct. Funct. Bioinf.* **2007**, *66*, 630–645.
- [21] H. Chen, H.-X. Zhou, *Proteins Struct. Funct. Bioinf.* **2005**, *61*, 21–35.
- [22] M. M. Bradford, *Anal. Biochem.* **1976**, *72*, 248–254.
- [23] S. Iqbal, Z. M. Khalid, K. A. Malik, *Lett. Appl. Microbiol.* **1995**, *21*, 176–179.
- [24] U. K. Laemmli, *Nature* **1970**, *227*, 680–685.
- [25] A. Shevchenko, M. Wilm, O. Vorm, M. Mann, *Anal. Chem.* **1996**, *68*, 850–858.
- [26] N. V. Gogichaeva, T. Williams, M. A. Alterman, *J. Am. Soc. Mass Spectrom.* **2007**, *18*, 279–284.
- [27] S. F. Altschul, T. L. Madden, A. A. Schäffer, J. Zhang, Z. Zhang, W. Miller, D. J. Lipman, *Nucleic Acids Res.* **1997**, *25*, 3389–3402.
- [28] W. Kabsch, *Acta Crystallogr. Sect. D Biol. Crystallogr.* **2010**, *66*, 125–132.
- [29] P. Evans, *Acta Crystallogr. Sect. D Biol. Crystallogr.* **2006**, *62*, 72–82.
- [30] P. Emsley, K. Cowtan, *Acta Crystallogr. Sect. D Biol. Crystallogr.* **2004**, *60*, 2126–2132.
- [31] P. D. Adams, P. V. Afonine, G. Bunkóczi, V. B. Chen, I. W. Davis, N. Echols, J. J. Headd, L.-W. Hung, G. J. Kapral, R. W. Grosse-Kunstleve, A. J. McCoy, N. W. Moriarty, R. Oeffner, R. J. Read, D. C. Richardson, J. S. Richardson, T. C. Terwilliger, P. H. Zwart, *Acta Crystallogr. Sect. D Biol. Crystallogr.* **2010**, *66*, 213–221.
- [32] G. N. Murshudov, P. Skubák, A. A. Lebedev, N. S. Pannu, R. A. Steiner, R. A. Nicholls, M. D. Winn, F. Long, A. A. Vagin, *Acta Crystallogr. Sect. D Biol. Crystallogr.* **2011**, *67*, 355–367.
- [33] A. J. McCoy, R. W. Grosse-Kunstleve, P. D. Adams, M. D. Winn, L. C. Storoni, R. J. Read, *J. Appl. Crystallogr.* **2007**, *40*, 658–674.
- [34] V. B. Chen, W. B. Arendall III, J. J. Headd, D. A. Keedy, R. M. Immormino, G. J. Kapral, L. W. Murray, J. S. Richardson, D. C. Richardson, *Acta Crystallogr. Sect. D Biol. Crystallogr.* **2010**, *66*, 12–21.

---

Received: November 19, 2013

Published online on January 17, 2014